First-Principles Study of Hydrogen Trapping and Diffusion Mechanisms in Vanadium Carbide with Connecting Carbon Vacancies

Article *in* International Journal of Hydrogen Energy · October 2024

DOI: 10.1016/j.ijhydene.2024.10.150

First-Principles Study of Hydrogen Trapping and Diffusion Mechanisms in Vanadium Carbide with Connecting Carbon Vacancies

Linxian Li,[a] Huifang Lan,[a], Shuai Tang,*[a] Haile Yan,[b] Fengliang Tan,[c] Sybrand van der Zwaag ,[d] Qing Peng,*[e,f,g] Zhenyu Liu[a] and Guodong Wang[a]

[a] *State Key Lab of Rolling and Automation, Northeastern University, Shenyang 110819, China.*
[b] *School of Materials Science and Engineering, Northeastern University, Shenyang 110819, China*
[c] *School of Materials and Environmental Engineering, Hunan University of Humanities, Science and Technology, Loudi 417000, China*
[d] *Novel Aerospace Materials Group, Faculty of Aerospace Engineering, Delft University of Technology, 2629 HS, Delft, Netherlands*
[e] *State Key Laboratory of Nonlinear Mechanics, Institute of Mechanics, Chinese Academy of Sciences, Beijing 100190, China.*
[f] *Guangdong Aerospace Research Academy, Guangzhou 511458, China*
[g] *Xinyan Semi Technology Co. Ltd, Wuhan, 430075, China*

**Corresponding authors:*

Shuai Tang, Email: tangshuai@ral.neu.edu.cn; Phone(o): +86 (24)-83672773

Qing Peng, Email: pengqing@imech.ac.cn; Phone(o): +86 (10)-82544239

Abstracts

Understanding the trapping and diffusion mechanism of hydrogen in vanadium carbide (VC) precipitates is crucial for exploring the issue of hydrogen embrittlement in steel. Although there is widespread consensus that VC can trap hydrogen, the mechanism by which hydrogen diffuses into VC is still unclear. In this study, we used first-principles calculation methods to study the influence of different spacings of Carbon vacancies on the trapping and diffusion of hydrogen in VC. The increase in the number of C vacancies makes it easier for vacancies to trap hydrogen, and hydrogen tend to fill up C vacancies. The diffusion of hydrogen into VC only occurs via neighboring C vacancies at 0.295 nm (connecting vacancies), leading to a diffusion barrier of 0.63~0.78 eV. This is consistent with experimental results and validates the experimental speculation that the diffusion of hydrogen in VC requires a connecting C vacancy grid.

Keywords: DFT calculation, VC precipitates, Hydrogen trap, Hydrogen diffusion

1. Introduction

High-strength steel continues to be the primary material for automotive bodies due to its excellent mechanical properties, formability, low price and readiness for corrosion protection treatments[1-5]. However, as steel strength increases, steels in general show a reduced resistance to hydrogen embrittlement [6,7] Research has demonstrated that [8-10] the aggregation of diffusible hydrogen to lattice defects such as grain boundaries and voids is the primary cause of hydrogen embrittlement. And second phases in crystal defects, such as precipitates and retained austenite, can be used to stop this long-range diffusion as they are effective hydrogen traps [11-15]. In automotive steel design carbide precipitates are widely used because they can greatly reduce the amount of matrix accumulated hydrogen and at the same time improve the (quasi-static) mechanical properties [16-20]. Of all the carbides, vanadium carbide (VC) is the most commonly used carbide in high-strength steel and can be present at levels up to 1.1 volume fraction and their presence has been shown to reduce the hydrogen embrittlement sensitivity significantly [21-26].

There are still a lot of controversies about the actual hydrogen trapping due to VC precipitates, both at the steel-precipitate interface and in the interior of precipitates. Takahashi initially proposed that the misfit dislocation core at the Fe/V_4C_3 semi-coherent interface was a deep hydrogen trap. However, subsequent studies highlighted the significance of the carbon (C) vacancy on the (001) surface of the V_4C_3 precipitate as of the strongest hydrogen trapping site [27,28]. Based on a detailed atom probe tomography (APT) analysis, Chen found that hydrogen is trapped in the interior of VC precipitates, and the measurements also revealed that the ratio of Vanadium to Carbon is roughly 4: 3, i.e. the carbides have a very high concentration of C vacancies [29-32]. Samanta [33] also discovered that in non-stoichiometric $NbC_{0.83}$, hydrogen atoms are trapped by C vacancies within NbC, instead of being trapped at the interface. Liu [34] compared the hydrogen trapping capabilities of TiC and (Ti, Mo)C and found that the addition of Mo increases the number of C vacancies in TiC, facilitating hydrogen entry into the carbide and enabling greater hydrogen trapping capacity.

Computational atomistic studies also emphasized the critical role of the C vacancy for hydrogen trapping due to its remarkably low hydrogen solution energy in VC [35-38]. Salehin [39] found that a lower carbon concentration in carbides allows them to trap more hydrogen atoms. Moreover, C vacancies at the VC interface can further enhance the hydrogen trapping ability of the trap [40,41]. The energy barrier for hydrogen diffusion from the α-Fe matrix to the C vacancy near

the interface (0.24 eV) is also much lower than that for hydrogen diffusion into the defect-free VC (2.13 eV) [42]. For the trapping of C vacancies at the interface, both experimental [27,43] and theoretical calculations [42,44,45] are considered to be feasible. Taniguchi [46] found a positive correlation between the amount of captured hydrogen in martensitic steels and the product of the carbide interfacial area and the concentration of C vacancies. Moreover, first-principles calculations have shown that the hydrogen capture energy of C vacancies at the interface is greater than in the Fe matrix. However, for hydrogen trapping within the carbide interiors, this has only been observed experimentally [29,47,48], and information regarding specific hydrogen trapping and diffusion mechanisms within carbide precipitates is still very scarce. A high binding energy in itself does not create an effective hydrogen binding trap, but a high diffusion coefficient is crucial for the hydrogen atoms to be able to reach vacancies located well within the actual precipitate [49]. It has been shown that the diffusion barrier of hydrogen atoms decreases with vacancy concentration, but the diffusion barrier is still high (the lowest is 2.12 eV) due to the C vacancies dis connecting (there are other C atoms between two C vacancies) [50]. The experimental studies suggest that diffusion of hydrogen atoms into the interior of carbides may require a continuous lattice of C vacancies [51,52]. Research is still scarce on how hydrogen atoms diffuse to the trapping sites within VC and their state of trapping.

In this paper, a mechanistic study of hydrogen trapping and diffusion behavior of different spacing C vacancies in the VC lattice is carried out using first-principles calculations, and the intrinsic mechanisms affecting the hydrogen diffusion barrier is analyzed.

2. Theoretical methods

To this aim first-principles calculations of the Vienna ab initio simulation package (VASP) [53] based on density functional theory have been performed. The calculations are performed for the situation at 0K and no correction are made to estimate the behaviour at room temperature or above, The electron-ion interactions and the exchange-correlation potential were treated employing the projector augmented wave (PAW) [54] and the generalized gradient approximation (GGA) [55] within the Perdew-Burke-Ernzerhof (PBE) [56] method, respectively. A plane wave cutoff energy of 520 eV was employed in all calculations. The supercell geometry and atomic positions of 2×2×2 VC supercells were relaxed, with the force and energy convergence criteria set at 0.01 eV/Å and 10^{-5} eV/cell, respectively. A 4×4×4 k-point mesh, following the Monkhorst-Pack [57] method, was

used for Brillouin zone sampling of VC supercells. The diffusion energy barrier of the hydrogen atom in VC was calculated by using the climbing image nudged elastic band (CINEB) method [58]. In addition, crystal structure visualization was achieved using VESTA software [59].

The ease of forming the *n*th C vacancy is described by the vacancy formation energy ($E_{\mathrm{f}}^{n\mathrm{Vac}}$), which is defined as:

$$E_{\mathrm{f}}^{n\mathrm{Vac}} = E_{n\mathrm{Vac}} + \mu_{\mathrm{C}} - E_{(n-1)\mathrm{Vac}} \quad (1)$$

Where $E_{n\mathrm{vac}}$ is the energy of the VC supercell with *n* C vacancies, and μ_{C} is the average energy of each C atom in graphite. Negative vacancy formation energy means that the *n*th C vacancy is easy to generate.

The solubility of *n*th hydrogen atom in the *m* C vacancies can be described by the solution energy ($E_{\mathrm{sol}}^{m\mathrm{Vac},n\mathrm{H}}$), which corresponds to the ability of the carbide to trap hydrogen atoms from the Fe matrix. This is defined as:

$$E_{\mathrm{sol}}^{m\mathrm{Vac},n\mathrm{H}} = \left(E_{m\mathrm{Vac},n\mathrm{H}} - E_{m\mathrm{Vac},(\mathrm{n}-1)\mathrm{H}}\right) - (E_{\mathrm{H}} - E_{\mathrm{Fe}}) \quad (2)$$

Where E_H is the system energy of Fe supercell when a single hydrogen atom occupies the most stable site (tetrahedral interstitial between the centers of four Fe atoms) [60]. E_{Fe} is the system energy of Fe supercell without hydrogen atom, and $E_{m\mathrm{Vac},n\mathrm{H}}$ is the system energy of VC supercell with *n* hydrogen atoms in the presence of *m* C vacancies. A negative solution energy indicates that the system can trap *n* hydrogen atoms, while a positive value means that the system can trap up to *n*-1 hydrogen atoms.

3. Results and discussion

Before conducing the calculations for hydrogen trapping and diffusion at vacancies, the e lattice constant of the defect free VC crystal was calculated and found to be 4.157 Å. This value closely aligns with both the experimental (4.15 Å [61]) and other theoretical (4.160 Å [62], 4.177 Å [63]) values. Subsequently, the formation energy of single carbon vacancies and double vacancies was considered. The ratios of V and C atoms in these two models are 32:31 and 16:15 respectively, implying that the level of carbon vacancies is still below the commonly observed carbide V_4C_3. For dual vacancies, different carbon vacancy distances were taken into account, their configurations are showed in Fig. 1. The vacancy formation energy of a solitary C vacancy is -1.03 eV. Considering the formation energy of the second C vacancy, it becomes apparent that with the exception of the configuration having an inter-vacancy distance of 4.16 Å, the vacancy formation energies for all the

other configurations are negative. The negative C vacancy formation energy indicates ease of formation for such configurations. Therefore, in subsequent calculations, configurations with a vacancy distance of 4.16 Å between the two vacancies are not taken into consideration.

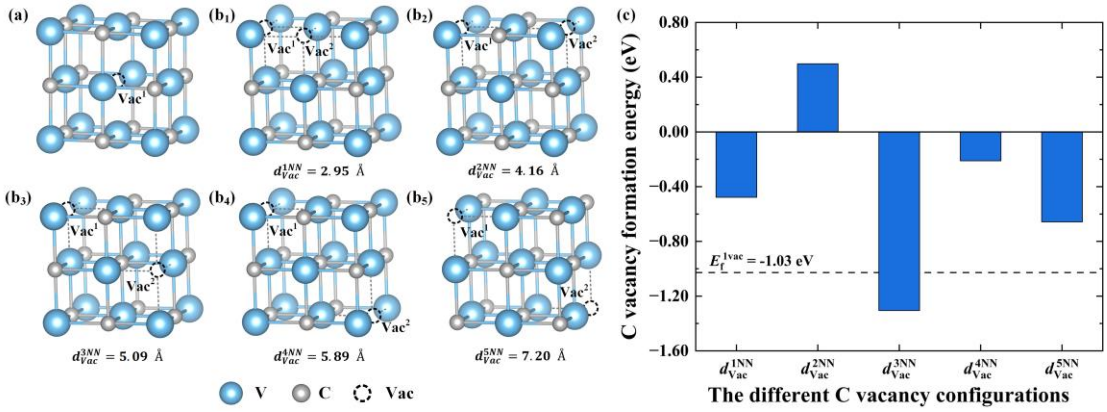

Fig. 1 Configurations of VC containing C vacancies and corresponding hydrogen trapping. (a) A single C vacancy. (b_1-b_5) Two C vacancies at different distances. (c) Formation energies of vacancies in different configurations, the dashed line indicates the formation energy of a single C vacancy.

Subsequently, the maximum hydrogen trapping number of a single C vacancy is calculated and the results are shown in Fig. 2(a). As the number of trapped hydrogen atoms increases, the hydrogen atoms are symmetrically distributed around the C vacancy and not in the center of the C vacancy. But they all have positive solvation energies. A single C vacancy can only trap one hydrogen atom stably, which is consistent with the result reported in the literature [49]. The hydrogen trapping of the two C vacancies is shown in Fig. 2(b). If neighboring C vacancies exist, the solution energy of a single hydrogen atom will be further reduced, and the solution energies of the second hydrogen atom is lower than that of one hydrogen atom in a single C vacancy. This indicates that the presence of neighboring C vacancies can enhance the hydrogen trapping ability of C vacancies, and hydrogen atoms tend to fill all C vacancies.

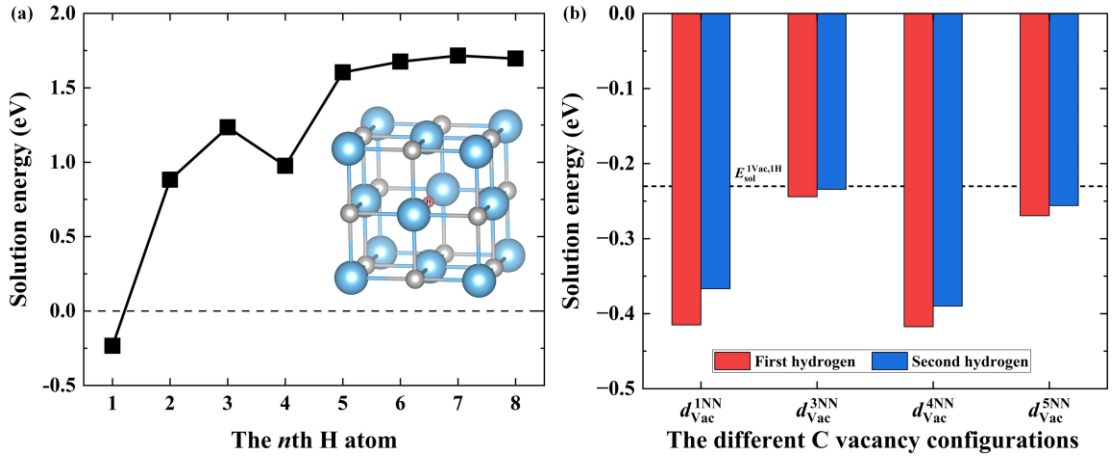

Fig. 2 Tydrogen trapping behavior of single C vacancy and double C vacancies. (a) Number of hydrogen trapped in a single vacancy. (b) Solution energy of hydrogen in double C vacancies.

The diffusivity of hydrogen atoms within the VC structure containing C vacancies is a key condition determining whether the VC can act as a stable trap capturing a significant number of hydrogen atoms. Thus, an analysis of hydrogen diffusion in VC is essential. Hydrogen diffusion in a perfect VC is discussed in the Supplementary Material (Fig. S1). Hydrogen atoms alternate between two diffusion paths in a perfect VC, with energy barriers of 0.17 eV and 0.32 eV, respectively, making the highest energy barrier for hydrogen diffusion 0.32 eV. To put the effect of the carbon vacancy on hydrogen diffusion in a proper context, the energy barrier of hydrogen atom diffusing from the trigonal interstitial of the third nearest neighbor (Tri-V^{3NN}) of C vacancy to C vacancy (Tri-V^{3NN}→Tri-V^{2NN}→Vac/Tri-V^{1NN}) and the energy barrier of hydrogen atom escaping from C vacancy to the Tri-V^{3NN} site (Vac/Tri-V^{1NN}→Tri-V^{2NN}→Tri-V^{3NN}) was studied. The diffusion energy barrier and path of hydrogen atom are shown in Fig. 3. The presence of a C vacancy has a minimal impact on the energy barrier for hydrogen atom diffusion from Tri-V^{3NN} site to Tri-V^{2NN} site ($E_{\mathrm{diff}}^{\mathrm{in},1}$). C vacancy primarily influences the energy barrier for hydrogen atoms diffusing from the Tri-V^{2NN} site to the C vacancy ($E_{\mathrm{diff}}^{\mathrm{in},2}$). $E_{\mathrm{diff}}^{\mathrm{in}}$ is lower than the energy barrier for hydrogen diffusion in a perfect VC (0.32 eV). And $E_{\mathrm{diff}}^{\mathrm{in}}$ is lower than that of the hydrogen atom in α-Fe (0.09 eV [15]), Therefore, the C vacancy attracts hydrogen atoms to diffuse towards it. Furthermore, the escape energy barriers ($E_{\mathrm{diff}}^{\mathrm{out}} = \mathrm{Max}\{E_{\mathrm{diff}}^{\mathrm{Vac/Tri-V^{1NN}\rightarrow Tri-V^{2NN}}}, E_{\mathrm{diff}}^{\mathrm{Tri-V^{2NN}\rightarrow Tri-V^{3NN}}}\}$, the energy barrier for hydrogen atoms diffusing from the C vacancy to the Tri-V^{3NN} site) of stable hydrogen atoms are higher than those of hydrogen diffusion in perfect VC. In brief, the presence of a C vacancy, acting as a strong hydrogen trap, effectively reduces the energy barrier for the diffusion of

hydrogen atom into the C vacancy while raising its escape energy barrier. Therefore, it is difficult for hydrogen atoms diffusing from the Fe matrix into the interfacial C vacancy to escape from the C vacancies into the defect-free VC matrix.

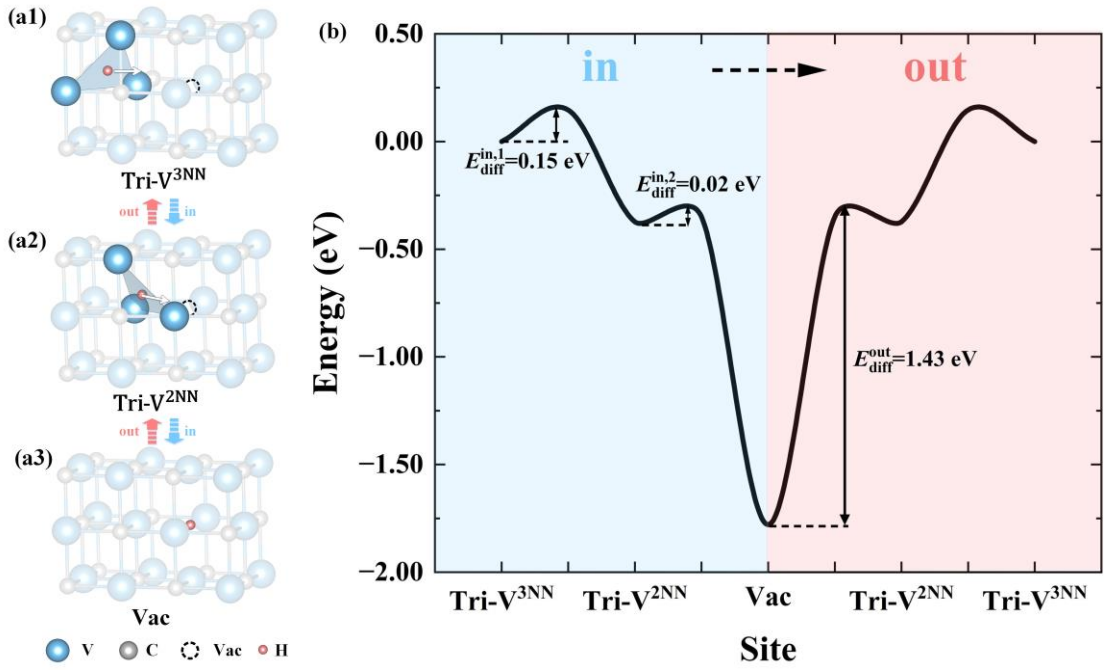

Fig. 3 Diffusion of hydrogen atoms near single C vacancy. The diffusion path (a1-a3) and energy barrier diagram (b) of hydrogen atom diffusing into and escaping from C vacancy.

Since it is difficult for hydrogen atoms to diffuse through the path mentioned above, hydrogen diffusion through neighboring C vacancies is considered, as shown in Fig. 4. The results show that the diffusion energy barriers for hydrogen are generally high (>2.1 eV) across all configurations except for the configuration with a vacancy spacing of 2.95 Å (0.63 eV). Therefore, if a hydrogen atom diffuses inside a carbide, it prefers to move through connected C vacancy path with a spacing of 2.95 Å. Similarly, if hydrogen atoms escape from the carbide, they favor the same connected C vacancy pathway. The energy required for hydrogen escape can be measured via Thermal Desorption Spectroscopy (TDS) experiments [64-68], making it possible to compare the calculated diffusion barriers with TDS experimental values. The results show that the diffusion energy barrier for a single hydrogen atom through the nearest neighboring C vacancy (0.63 eV) aligns with TDS experiments (52-67 kJ/mol [22], 53-72 kJ/mol [69], 87.3 kJ/mol [70]). This further confirms that hydrogen can diffuse into the carbide interior through connected C vacancies.

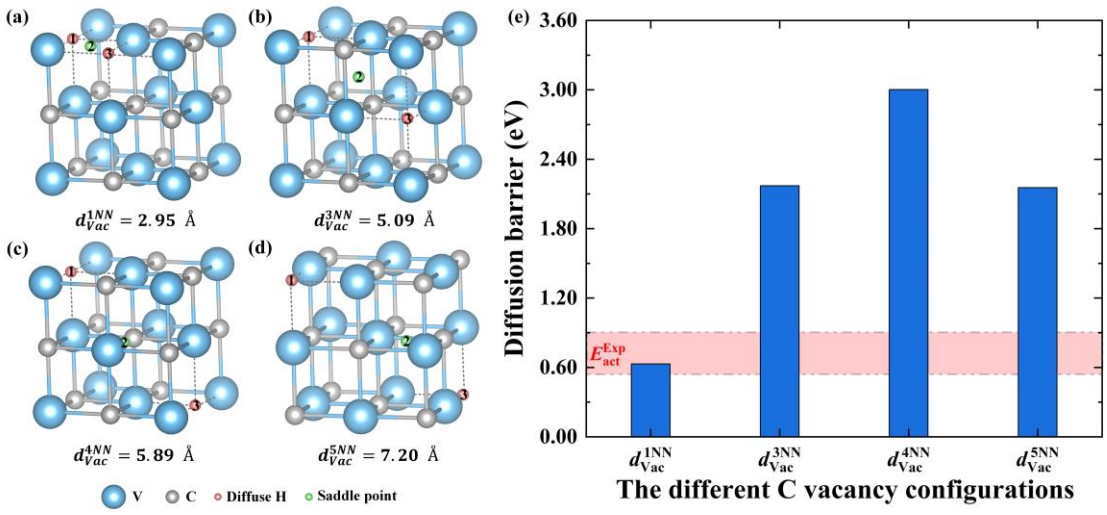

Fig. 4 Diffusion of hydrogen atoms occurs through the near-neighbor C vacancy. (a) Diffusion path and (b) diffusion energy barrier for hydrogen atom.

The trapping and diffusion of hydrogen in the presence of three C vacancies with a spacing of 2.95 Å in the VC are considered next, and the configuration is obtained by searching for the third most stable C vacancy on the basis of the configuration of the two C vacancies with a spacing of 2.95 Å, which is shown in Fig. 5(a). It was found that the formation energy of the third Carbon vacancy is -0.71eV, implying that this configuration is also easy to generate. The hydrogen trapping ability from a single vacancy to three vacancies was compared in Fig. 5(b). The results indicate that the hydrogen trapping ability of C vacancy for the first hydrogen increases with the rise in C vacancy concentration. Combining the hydrogen trapping ability of the three C vacancy configurations, it can be found that hydrogen atoms tend to occupy the C vacancy completely. This further emphasizes the importance of connecting vacancies.

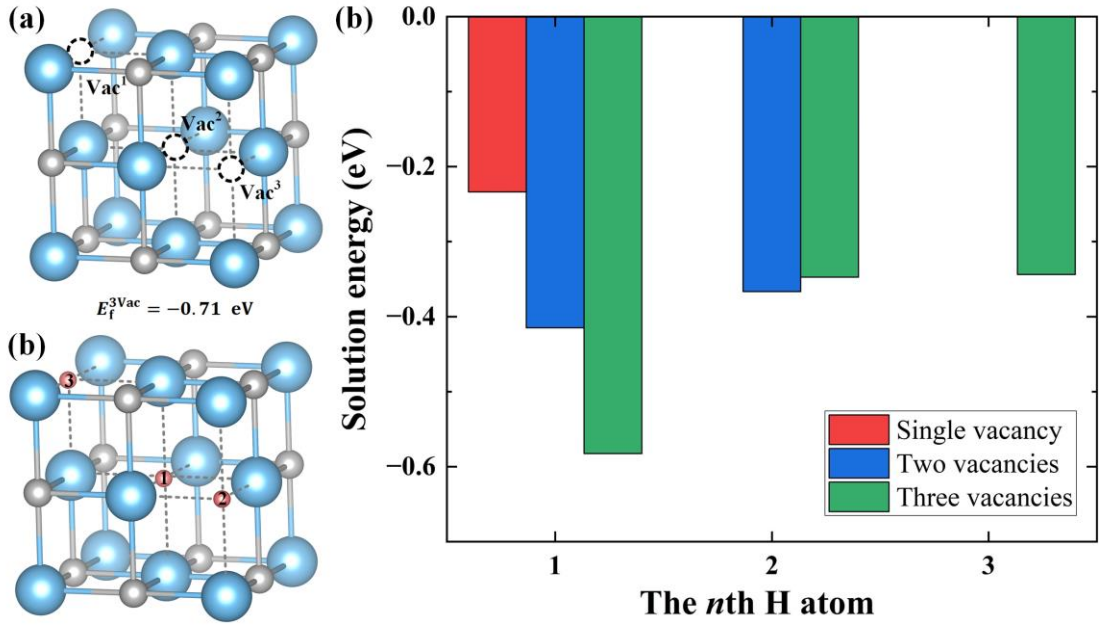

Fig. 5 Hydrogen trapping in three C vacancies. (a) Three C vacancies configurations, (b) hydrogen trapping order in three vacancies configuration and (c) hydrogen trapping in the C vacancies.

Following this, the diffusion of a single Hydrogen atom between vacancies along $Vac^3 \rightarrow Vac^2 \rightarrow Vac^1$ pathway was calculated, which is shown in Fig. 6. The maximum diffusion energy barrier for this pathway is calculated to be 0.78eV (75 kJ/mol), which is still in line with the results achieved from the TDS experiment (52.0-87.3 kJ/mol). And the case of hydrogen atoms undergoing jump diffusion was also considered, with the path $Vac^3 \rightarrow Vac^1$. However, it was found that hydrogen atoms could not diffuse directly from the Vac^3 site to the Vac^1 site, and that hydrogen atoms had to pass through the Vac^2 site in order to diffuse to the Vac^1 site.

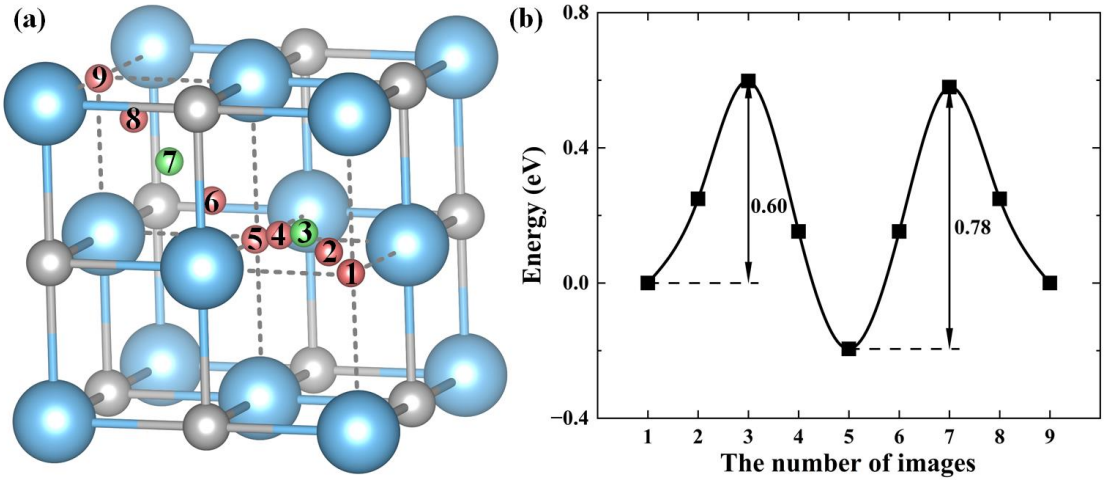

Fig. 6 Hydrogen diffusion in three C vacancies. the diffusion path (a) and energy barriers (b) of single hydrogen.

Next is the diffusion of hydrogen atoms when there are two hydrogen atoms in a configuration with three C vacancies, as shown in Fig. 7(a-d). There are two cases: the first one is the jump diffusion of hydrogen atoms through the vacancies with a spacing of 5.09 Å, and the path is $Vac^3 \rightarrow Vac^1$. The second one is the diffusion of hydrogen atoms through the nearest-neighboring vacancies with a spacing of 2.95 Å, and the paths are $Vac^2 \rightarrow Vac^1$, and $Vac^3 \rightarrow Vac^2$. The end result from both diffusion methods is the same. The diffusion energy barrier in the first case is 1.34eV, while in the second case, it is 0.77eV. Although the hydrogen atom can diffuse by jump diffusion through the first diffusion mode, its energy barrier is still high, which implies that diffusion of hydrogen still occurs through nearest-neighbour C vacancies. This observation may explain the ongoing debate about the APT results related to hydrogen trapping sites in VC precipitates. Variations in the experimental procedures in the mentioned literature have eventually led to changes in the Carbon vacancy concentration in VC. When consecutive Carbon vacancies exist, the higher the concentration of C vacancies, the easier it is for hydrogen atoms to diffuse from α-Fe into VC precipitates and the higher the number of hydrogen atoms that are trapped inside the carbide.

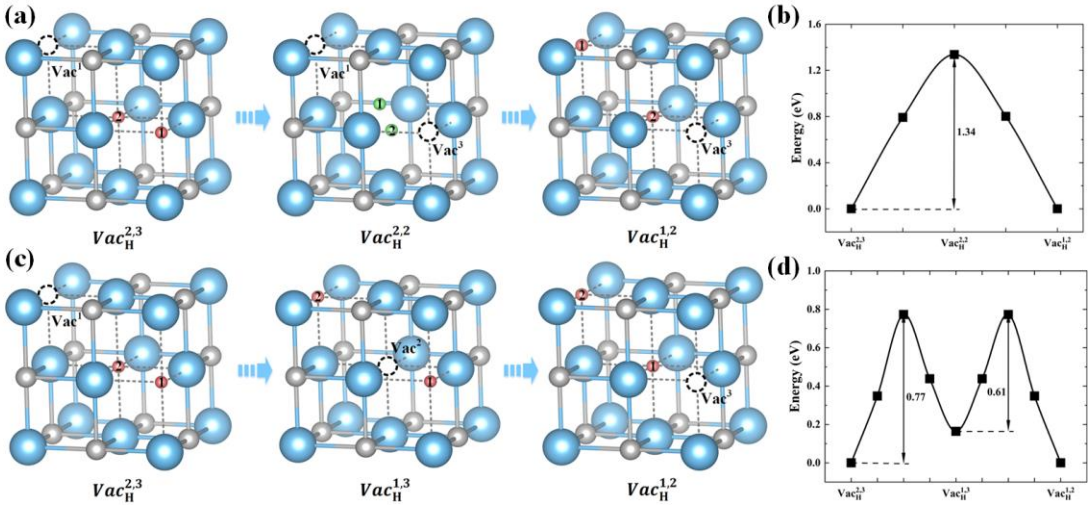

Fig. 7 Hydrogen diffusion in three C vacancies. The first diffusion path (a) and energy barrier (b) of two hydrogen atoms; the second diffusion path (c) and energy barrier (d) of two hydrogen atoms.

In order to understand the reasons affecting the significant differences in the diffusion energy barriers of hydrogen atoms at different vacancy spacings, Electron Localization Function (ELF) analysis was carried out and the results are shown in Fig. 8. The results show that the ELF values near the vacancies fluctuate around 0.5 (uniform electron gas state), which does not change with the

vacancy spacing. For a vacancy spacing of 2.95 Å, there is a connecting uniform electron gas between the two vacancies and the saddle point of the diffusion path is also on this channel, which makes the obstruction for hydrogen atoms to diffuse through this channel to occur lower. This is not the case for other vacancy spacing configurations, where the charge density between the vacancies fluctuates more, which leads to a rapid increase in the corresponding diffusion energy barrier.

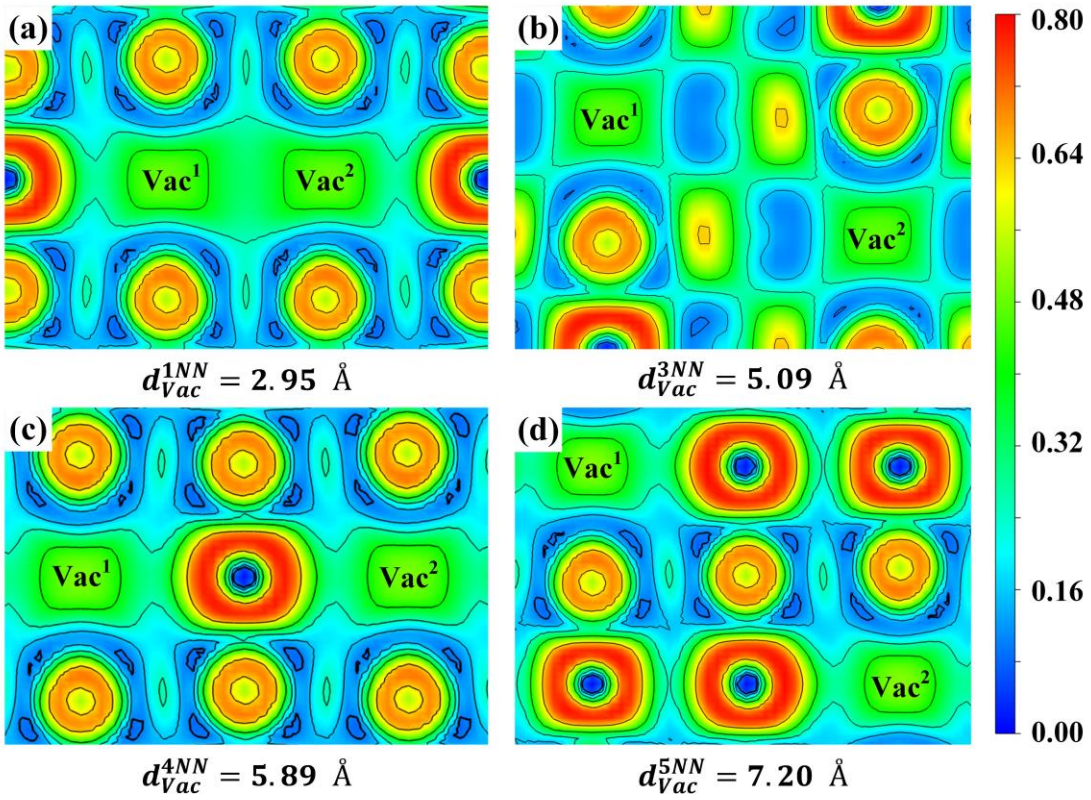

Fig. 8 ELF plots at different vacancy spacings. (a) 2.95 Å, (b) 5.09 Å, (c) 5.89 Å, (d) 7.20 Å.

4. Conclusions

In this paper, hydrogen trapping and diffusion in VC precipitates are investigated by first-principles calculations. The results show that hydrogen atoms can only diffuse from the Fe matrix to the interior of the VC precipitates through a connecting network of C vacancies (C vacancies with a spacing of 2.95 Å). And increasing vacancy concentration, the hydrogen trapping ability of C vacancies is enhanced and hydrogen atoms tend to occupy all C vacancies. The energy barrier for hydrogen atom diffusion through this pathway is 0.63-0.78 eV (60-75 kJ/mol), which is in good agreement with the results obtained by TDS (52.0-87.3 kJ/mol). Moreover, hydrogen atoms can only diffuse through the nearest neighboring C vacancies, and no long range jump diffusion can

occur. The channels formed by the uniform electron gas between the nearest-neighbor vacancies are responsible for the low diffusion energy barrier. Therefore, the connectivity of C vacancies is essential for hydrogen diffusion into the carbide and the substantial capture of hydrogen by VC precipitates.

Acknowledgments

S. T. gratefully acknowledges the financial support of National Natural Science Foundation of China (Grant Nos. 52175293 and 51774083). Q. P. would like to acknowledge the support provided by National Natural Science Foundation of China (Grant No. 12272378), Open Research Fund of State Key Laboratory of Rolling and Automation, Northeastern University (2022RALKFKT006), Strategic Priority Research Program of Chinese Academy of Sciences (Grant No. XDB0620103), High-level Innovation Research Institute Program of Guangdong Province (Grant No. 2020B0909010003). The authors sincerely thank Dr. Marcel H.F. Sluiter (Mechanical Engineering Materials Science and Engineering, Delft University of Technology) for valuable suggestions and revisions.

References:

[1] Omiya M, Arakawa S, Yao Z, Muramatsu M, Nishi S, Takada K, et al. Influence of strength and notch shape on crack initiation and propagation behavior of advanced high strength steel sheets. Eng Fract Mech 2022; 271:108573. https://doi.org/10.1016/j.engfracmech.2022.108573.

[2] Yaghoobi F, Jamaati R, Aval HJ. Resistance spot welding of high-strength DP steel and nano/ultrafine-grained IF steel sheets. Mater Chem Phys 2022; 281:125909. https://doi.org/10.1016/j.matchemphys.2022.125909.

[3] Li H, Venezuela J, Zhou Q, Luzin V, Yan M, Shi Z, et al. Hydrogen-induced delayed fracture of a 1180 MPa martensitic advanced high-strength steel under U-bend loading. Mater Today Commun 2021; 26:101887. https://doi.org/10.1016/j.mtcomm.2020.101887.

[4] Gong P, Turk A, Nutter J, Yu F, Wynne B, Rivera-Diaz-del-Castillo P, et al. Hydrogen embrittlement mechanisms in advanced high strength steel. Acta Mater 2022; 223:117488. https://doi.org/10.1016/j.actamat.2021.117488.

[5] Rossini M, Spena PR, Cortese L, Matteis P, Firrao D. Investigation on dissimilar laser welding of advanced high strength steel sheets for the automotive industry. Mater Sci Eng A 2015; 628:288-96. https://doi.org/10.1016/j.msea.2015.01.037.

[6] Bhadeshia HKDH. Prevention of Hydrogen Embrittlement in Steels. ISIJ Int 2016; 56:24-36. https://doi.org/10.2355/isijinternational.ISIJINT-2015-430.

[7] Koyama M, Akiyama E, Lee Y, Raabe D, Tsuzaki K. Overview of hydrogen embrittlement in high-Mn steels. Int J Hydrogen Energy 2017; 42:12706-23.

https://doi.org/10.1016/j.ijhydene.2017.02.214.
[8] Takano N. Hydrogen diffusion and embrittlement in 7075 aluminum alloy. Mater Sci Eng A 2008; 483:336-9. https://doi.org/10.1016/j.msea.2006.08.144.
[9] Song J, Curtin WA. Atomic mechanism and prediction of hydrogen embrittlement in iron. Nat Mater 2013; 12:145-51. https://doi.org/10.1038/nmat3479.
[10] Lassila DH, Birnbaum HK. The effect of diffusive hydrogen segregation on fracture of polycrystalline nickel. Acta Metall 1986; 34:1237-43. https://doi.org/10.1016/0001-6160(86)90010-6.
[11] Wei FG, Tsuzaki K. Quantitative analysis on hydrogen trapping of TiC particles in steel. Metall Mater Trans A 2006; 37:331-53. https://doi.org/10.1016/10.1007/s11661-006-0004-3.
[12] Wei F, Hara T, Tsuzaki K, 2011. Nano-Preciptates Design with Hydrogen Trapping Character in High Strength Steel. Springer Berlin Heidelberg, Berlin, Heidelberg, pp. 87-92. https://doi.org/10.1007/978-3-642-17665-4_11.
[13] Wallaert E, Depover T, Arafin M, Verbeken K. Thermal Desorption Spectroscopy Evaluation of the Hydrogen-Trapping Capacity of NbC and NbN Precipitates. Metall Mater Trans A 2014; 45:2412-20. https://doi.org/10.1007/s11661-013-2181-1.
[14] Nagao A, Martin ML, Dadfarnia M, Sofronis P, Robertson IM. The effect of nanosized (Ti, Mo)C precipitates on hydrogen embrittlement of tempered lath martensitic steel. Acta Mater 2014; 74:244-54. https://doi.org/10.1016/j.actamat.2014.04.051.
[15] Nazarov R, Hickel T, Neugebauer J, Mrovec M, Elsässer C, Di Stefano D. First-principles investigation of hydrogen interaction with TiC precipitates in α-Fe. Phys Rev B 2016; 93:184108. https://doi.org/10.1103/PhysRevB.93.184108.
[16] Dos Santos TAA, de Lima MM, Dos Santos DS, Buono VTL. Effect of nano Nb and V carbides on the hydrogen interaction in tempered martensitic steels. Int J Hydrogen Energy 2022; 47:1358-70. https://doi.org/10.1016/j.ijhydene.2021.10.051.
[17] Seo HJ, Heo Y, Kim JN, Lee J, Choi S, Lee CS. Effect of V/Mo ratio on the evolution of carbide precipitates and hydrogen embrittlement of tempered martensitic steel. Corros Sci 2020; 176:108929. https://doi.org/10.1016/j.corsci.2020.108929.
[18] Zhang S, Wan J, Zhao Q, Liu J, Huang F, Huang Y, et al. Dual role of nanosized NbC precipitates in hydrogen embrittlement susceptibility of lath martensitic steel. Corros Sci 2020; 164:108345. https://doi.org/10.1016/j.corsci.2019.108345.
[19] Depover T, Verbeken K. The effect of TiC on the hydrogen induced ductility loss and trapping behavior of Fe-C-Ti alloys. Corros Sci 2016; 112:308-26. https://doi.org/10.1016/j.corsci.2016.07.013.
[20] Lin L, Li B, Zhu G, Kang Y, Liu R. Effect of niobium precipitation behavior on microstructure and hydrogen induced cracking of press hardening steel 22MnB5. Mater Sci Eng A 2018; 721:38-46. https://doi.org/10.1016/j.msea.2018.02.021.
[21] Liu H, Zhou H, Luo G, Zheng P. The influence of deuterium ions on the deuterium permeation and retention behavior in V-4Cr-4Ti alloy under plasma loading. J Nucl Mater 2021; 554:153071. https://doi.org/10.1016/j.jnucmat.2021.153071.
[22] Depover T, Verbeken K. Evaluation of the effect of V4C3 precipitates on the hydrogen induced mechanical degradation in Fe-C-V alloys. Mater Sci Eng A 2016; 675:299-313. https://doi.org/10.1016/j.msea.2016.08.053.
[23] Seo HJ, Kim JN, Jo JW, Lee CS. Effect of tempering duration on hydrogen embrittlement of

vanadium-added tempered martensitic steel. Int J Hydrogen Energy 2021; 46:19670-81. https://doi.org/10.1016/j.ijhydene.2021.03.109.

[24] Li Y, Zhang X, Wu T. First-principles study on the dissolution and diffusion behavior of hydrogen in carbide precipitates. Int J Hydrogen Energy 2021; 46:22030-9. https://doi.org/10.1016/j.ijhydene.2021.04.056.

[25] Li L, Song B, Cai Z, Liu Z, Cui X. Effect of vanadium content on hydrogen diffusion behaviors and hydrogen induced ductility loss of X80 pipeline steel. Mater Sci Eng A 2019; 742:712-21. https://doi.org/10.1016/j.msea.2018.09.048.

[26] Tang S, Li L, Yan H, Jin J, Peng Q, Cai M, et al. Hydrogen trapping in vanadium carbide alloyed with transition metals. Nucl Mater Energy 2023; 36:101504. https://doi.org/10.1016/j.nme.2023.101504.

[27] Takahashi J, Kawakami K, Kobayashi Y. Origin of hydrogen trapping site in vanadium carbide precipitation strengthening steel. Acta Mater 2018; 153:193-204. https://doi.org/10.1016/j.actamat.2018.05.003.

[28] Takahashi J, Kawakami K, Tarui T. Direct observation of hydrogen-trapping sites in vanadium carbide precipitation steel by atom probe tomography. Scr Mater 2012; 67:213-6. https://doi.org/10.1016/j.scriptamat.2012.04.022.

[29] Chen Y, Haley D, Gerstl SSA, London AJ, Sweeney F, Wepf RA, et al. Direct observation of individual hydrogen atoms at trapping sites in a ferritic steel. Sci 2017; 355:1196-9. https://doi.org/10.1126/science.aal2418.

[30] Yu X, Thompson GB, Weinberger CR. Influence of carbon vacancy formation on the elastic constants and hardening mechanisms in transition metal carbides. J Eur Ceram Soc 2015; 35:95-103. https://doi.org/10.1016/j.jeurceramsoc.2014.08.021.

[31] Williams WS. Physics of transition metal carbides. Mater Sci Eng A 1988; 105:1-10. https://doi.org/10.1016/0025-5416(88)90474-0.

[32] Speich GR, Leslie WC. Tempering of steel. Metall Trans 1972; 3:1043-54. https://doi.org/10.1007/BF02642436.

[33] Samanta S, Gangavarapu S, Jayabalan B, Makineni SK, Dutta M, Singh SB. Atomic-scale investigation of H-trapping by fine NbC precipitates in a low C ferritic steel. Scr Mater 2023; 234:115537. https://doi.org/10.1016/j.scriptamat.2023.115537.

[34] Liu PY, Zhang B, Niu R, Lu SL, Huang C, Wang M, et al. Engineering metal-carbide hydrogen traps in steels. Nat Commun 2024; 15:724. https://doi.org/10.1038/s41467-024-45017-4.

[35] Kawakami K, Matsumiya T. Numerical Analysis of Hydrogen Trap State by TiC and V4C3 in bcc-Fe. ISIJ Int 2012; 52:1693-7. https://doi.org/10.2355/isijinternational.52.1693.

[36] Echeverri Restrepo S, Di Stefano D, Mrovec M. Density functional theory calculations of iron - vanadium carbide interfaces and the effect of hydrogen. Int J Hydrogen Energy 2020; 45:2382-9. https://doi.org/10.1016/j.ijhydene.2019.11.102.

[37] Tang S, Li L, Peng Q, Yan H. First-principles insights into hydrogen trapping in interstitial-vacancy complexes in vanadium carbide. Phys Chem Chem Phys 2022; 24:20400-8. https://doi.org/10.1039/D2CP02425J.

[38] Li M, Ding W, Lei X, Lu X, Gan Z, Sun Y. Hydrogen trapping behavior in IVB-VB transition metal carbides. Mater Today Commun 2024; 40:109587. https://doi.org/10.1016/j.mtcomm.2024.109587.

[39] Salehin R, Thompson GB, Weinberger CR. Hydrogen trapping and storage in the group IVB-VIB

transition metal carbides. Mater Des 2022; 214:110399. https://doi.org/10.1016/j.matdes.2022.110399.

[40] Ma Y, Shi Y, Wang H. A first-principles study on the hydrogen trap characteristics of coherent nano-precipitates in α-Fe. Int J Hydrogen Energy 2020; 45:27941-9. https://doi.org/10.1016/j.ijhydene.2020.07.123.

[41] Kirchheim R. Changing the interfacial composition of carbide precipitates in metals and its effect on hydrogen trapping. Scr Mater 2019; 160:62-5. https://doi.org/10.1016/j.scriptamat.2018.09.043.

[42] Ma Y, Zhou S, He Y, Su Y, Qiao L, Gao L. Understanding the migration mechanism of hydrogen atom from the α-Fe matrix into nano-precipitates via DFT calculations. Phys Chem Chem Phys 2023; 25:29727-37. https://doi.org/10.1039/D3CP03499B.

[43] Takahashi J, Kawakami K, Sakiyama Y, Ohmura T. Atomic-scale observation of hydrogen trap sites in bainite–austenite dual-phase steel by APT. Mater Charact 2021; 178:111282. https://doi.org/10.1016/j.matchar.2021.111282.

[44] Hammer P, Romaner L, Razumovskiy VI. Hydrogen trapping in mixed carbonitrides. Acta Mater 2024; 268:119754. https://doi.org/10.1016/j.actamat.2024.119754.

[45] Song EJ, Baek S, Nahm SH, Suh D. Effects of Molybdenum Addition on Hydrogen Desorption of TiC Precipitation-Hardened Steel. Met Mater Int 2018; 24:532-6. https://doi.org/10.1007/s12540-018-0067-x.

[46] Taniguchi S, Kameya M, Kobayashi Y, Ito K, Yamasaki S. Hydrogen Trapping and Precipitation of Alloy Carbides in Molybdenum Added Steels and Vanadium Added Steels. ISIJ Int 2024; 64:1057-66. https://doi.org/10.2355/isijinternational.ISIJINT-2024-031.

[47] Malard B, Remy B, Scott C, Deschamps A, Chêne J, Dieudonné T, et al. Hydrogen trapping by VC precipitates and structural defects in a high strength Fe–Mn–C steel studied by small-angle neutron scattering. Mater Sci Eng A 2012; 536:110-6. https://doi.org/10.1016/j.msea.2011.12.080.

[48] Wallaert E, Depover T, Arafin M, Verbeken K. Thermal Desorption Spectroscopy Evaluation of the Hydrogen-Trapping Capacity of NbC and NbN Precipitates. Metall Mater Trans A 2014; 45:2412-20. https://doi.org/10.1007/s11661-013-2181-1.

[49] Sagar S, Sluiter MHF, Dey P. First - Principles study of hydrogen - Carbide interaction in bcc Fe. Int J Hydrogen Energy 2023. https://doi.org/10.1016/j.ijhydene.2023.09.222.

[50] Huang S, Tian J, Liu Y. Atomic study of hydrogen behavior in different vanadium carbides. J Nucl Mater 2021; 554:153096. https://doi.org/10.1016/j.jnucmat.2021.153096.

[51] Vandewalle L, Depover T, Verbeken K. Hydrogen trapping of carbides during high temperature gaseous hydrogenation. Int J Hydrogen Energy 2023; 48:32158-68. https://doi.org/10.1016/j.ijhydene.2023.04.348.

[52] Nguyen J, Glandut N, Jaoul C, Lefort P. Hydrogen insertion in substoichiometric titanium carbide. Int J Hydrogen Energy 2015; 40:8562-70. https://doi.org/10.1016/j.ijhydene.2015.05.009.

[53] A GK, B JF. Efficiency of ab-initio total energy calculations for metals and semiconductors using a plane-wave basis set. Comput Mater Sci 1996; 6:15-50. https://doi.org/10.1016/0927-0256(96)00008-0.

[54] Enkovaara J, Rostgaard C, Mortensen JJ, Chen J. Electronic structure calculations with GPAW: a real-space implementation of the projector augmented-wave method. J Phys Condens Matter 2010; 22:253202. https://doi.org/10.1088/0953-8984/22/25/253202.

[55] Perdew JP, Chevary JA, Vosko SH. Erratum: Atoms, molecules, solids, and surfaces: Applications of the generalized gradient approximation for exchange and correlation. Phys Rev B, Condensed

matter 1993; 48:4978. https://doi.org/10.1103/PhysRevB.48.4978.2.
[56] Perdew JP, Burke K, Ernzerhof M. Generalized Gradient Approximation Made Simple. Phys Rev Lett 1996; 77:3865-8. https://doi.org/10.1103/PhysRevLett.77.3865.
[57] Chadi DJ. Special points for Brillouin-zone integrations. Phys Rev B 1977; 16:1746-7. https://doi.org/10.1016/10.1103/PhysRevB.16.1746.
[58] Henkelman G, Jónsson H. A dimer method for finding saddle points on high dimensional potential surfaces using only first derivatives. J Chem Phys 1999; 111:7010-22. https://doi.org/10.1063/1.480097.
[59] Momma K, Izumi F. VESTA 3 for three-dimensional visualization of crystal, volumetric and morphology data. J Appl Crystallogr 2011; 44:1272-6. https://doi.org/10.1107/S0021889811038970.
[60] Counts WA, Wolverton C, Gibala R. First-principles energetics of hydrogen traps in α-Fe: Point defects. Acta Mater 2010; 58:4730-41. https://doi.org/10.1016/j.actamat.2010.05.010.
[61] Pflüger J, Fink J, Weber W, Bohnen KP, Crecelius G. Dielectric properties of TiCx, TiNx, VCx, and VNx from 1.5 to 40 eV determined by electron-energy-loss spectroscopy. Phys Rev B 1984; 30:1155-63. https://doi.org/10.1103/PhysRevB.30.1155.
[62] Liu H, Zhu J, Liu Y, Lai Z. First-principles study on the mechanical properties of vanadium carbides VC and V4C3. Mater Lett 2008; 62:3084-6. https://doi.org/10.1016/j.matlet.2008.01.136.
[63] Chen L, Li Y, Peng J, Sun L, Li B, Wang Z, et al. A comparable study of Fe//MCs (M = Ti, V) interfaces by first-principles method: The chemical bonding, work of adhesion and electronic structures. J Phys Chem Solids 2020; 138:109292. https://doi.org/10.1016/j.jpcs.2019.109292.
[64] Zhou Y, Wu W, Li J. Simultaneous improvement of hydrogen embrittlement resistance and tensile strength of quenching and partitioning steel through dense multiple interfaces. Int J Hydrogen Energy 2024; 58:1372-85. https://doi.org/10.1016/j.ijhydene.2024.01.270.
[65] Fang B, Hui W, Song H, Zhang Y, Zhao X, Xu L. Hydrogen embrittlement of a V+Nb-microalloyed medium-carbon bolt steel subjected to different tempering temperatures. Int J Hydrogen Energy 2024; 81:458-70. https://doi.org/10.1016/j.ijhydene.2024.07.321.
[66] Almeida LDS, Marques SC, Dos Santos DS. The influence of steelmaking processes on the hydrogen embrittlement of a tempered martensitic steel. Int J Hydrogen Energy 2024; 78:662-73. https://doi.org/10.1016/j.ijhydene.2024.06.251.
[67] Pinson M, Claeys L, Springer H, Bliznuk V, Depover T, Verbeken K. Investigation of the effect of carbon on the reversible hydrogen trapping behavior in lab-cast martensitic FeC steels. Mater Charact 2022; 184:111671. https://doi.org/10.1016/j.matchar.2021.111671.
[68] Lang F, Huang F, Yue J, Li L, Xu J, Liu J. Hydrogen trapping and hydrogen embrittlement (HE) susceptibility of X70 grade high-strength, acid-resistant, submarine pipeline steel with Mg treatment. J Mater Res Technol 2023; 24:623-38. https://doi.org/10.1016/j.jmrt.2023.03.011.
[69] Boot T, Suresh Kumar A, Eswara S, Kömmelt P, Böttger A, Popovich V. Hydrogen trapping and embrittlement of titanium- and vanadium carbide-containing steels after high-temperature hydrogen charging. J Mater Sci 2024; 59:7873-92. https://doi.org/10.1007/s10853-024-09611-7.
[70] Moshtaghi M, Maawad E, Bendo A, Krause A, Todt J, Keckes J, et al. Design of high-strength martensitic steels by novel mixed-metal nanoprecipitates for high toughness and suppressed hydrogen embrittlement. Mater Des 2023; 234:112323. https://doi.org/10.1016/j.matdes.2023.112323.